VOID STRUCTURE AND DENSITY CHANGE OF VANADIUM-BASE ALLOYS IRRADIATED IN THE DYNAMIC HELIUM CHARGING EXPERIMENT*

H. M. Chung, L. Nowicki, J. Gazda, and D. L. Smith (Argonne National Laboratory)

OBJECTIVE

The objective of this work is to determine void structure, distribution, and density changes of several promising vanadium–base alloys irradiated in the Dynamic Helium Charging Experiment (DHCE).

SUMMARY

Combined effects of dynamically charged helium and neutron damage on density change, void distribution, and microstructural evolution of V–4Cr–4Ti alloy have been determined after irradiation to 18–31 dpa at 425–600°C in the DHCE, and the results compared with those from a non–DHCE in which helium generation was negligible. For specimens irradiated to ≈18–31 dpa at 500–600°C with a helium generation rate of 0.4–4.2 appm He/dpa, only a few helium bubbles were observed at the interface of grain matrices and some of the Ti(O,N,C) precipitates, and no microvoids or helium bubbles were observed either in grain matrices or near grain boundaries. Under these conditions, dynamically produced helium atoms seem to be trapped in the grain matrix without significant bubble nucleation or growth, and in accordance with this, density changes from DHCE and non–DHCE (negligible helium generation) were similar for comparable fluence and irradiation temperature. Only for specimens irradiated to ≈31 dpa at 425°C, when helium was generated at a rate of 0.4–0.8 appm helium/dpa, were diffuse helium bubbles observed in limited regions of grain matrices and near ≈15% of the grain boundaries in densities significantly lower than those in the extensive coalescences of helium bubbles typical of other alloys irradiated in tritium–trick experiments. Density changes of specimens irradiated at 425°C in the DHCE were somewhat higher than those from non–DHCE irradiation. Microstructural evolution in V–4Cr–4Ti was similar for DHCE and non–DHCE except for helium bubble number density and distribution. As in non–DHCE, the irradiation–induced precipitation of ultrafine Ti_5Si_3 was observed for DHCE at >500°C but not at 425°C.

INTRODUCTION

Recent attention in the development of vanadium–base alloys for application in fusion reactor first wall and blanket structure has focused on V-4Cr-4Ti, an alloy reported to exhibit an excellent combination of mechanical and physical properties before and after irradiation.[1–6] One unresolved issue in the performance of the alloy, however, has been the effect of fusion–relevant simultaneous generation of helium and neutron damage (at a ratio of 4–5 appm helium/displacement per atom [dpa]) on density change and void swelling. Helium effects determined for other vanadium–base alloys by means of less fusion–relevant simulation approaches such as tritium-trick,[7–13] cyclotron-injection,[14–18] and boron-doping[18–21] techniques have been inconsistent with regard to concentration of helium bubbles on grain boundaries and the concomitant propensity for intergranular fracture. In the unique DHCE, the fusion–relevant helium–to–dpa ratio is simulated realistically by utilizing transmutation of controlled amounts of ^6Li and a predetermined amount of tritium–doped mother alloy immersed in $^6Li + {}^7Li$.[22–24] This report describes results of microstructural characterization and density measurement, primarily of V–4Cr–4Ti alloy specimens irradiated to 18–31 dpa at 425–600°C in the DHCE.

MATERIALS AND PROCEDURES

The elemental composition of the V–4Cr–4Ti alloy (ANL Identification BL–47), determined prior to irradiation, is given in Table 1. Postirradiation examination of other alloys listed in Table 1 (i.e., V–5Ti, V–3Ti–1Si, and V–8Cr–6Ti) was limited; unless pointed out specifically, all results reported in this study refer to V–4Cr–4Ti. Fabrication procedures of the alloy ingots and annealed plates and sheets have been reported

* Work supported by the U.S. Department of Energy, Office of Fusion Energy, under Contract W-31-109-Eng-38.

elsewhere.[25] TEM disks, punched from 0.3–mm–thick cold–worked sheets for use in investigating density change, void swelling behavior, and microstructural characteristics, were annealed at 1050°C in an ion–pumped high–vacuum system. The annealed material was ≈95% recrystallized and exhibited an average grain size of ≈14 μm. Phase structures of the alloy, characterized before and after irradiation in a non–DHCE (negligible helium generation), have been described in detail elsewhere.[4] The only secondary phase present in the as–annealed specimens was Ti(O,N,C), which is normally observed in titanium–containing vanadium alloys with O+N+C > 400 wppm.[26]

Table 1. Chemical composition of vanadium–base alloys

ANL ID	Nominal Composition (wt.%)	Impurity Composition (wppm) O	N	C	Si	S	P	Nb	Mo
BL-47	V–4.1Cr–4.3Ti	350	220	200	870	20	<40	<100	<100
BL-46	V–4.6Ti	305	53	85	160	10	<100	<100	–
BL-45	V–2.5Ti–1.0Si	345	125	90	9900	30	–	200	140
BL-49	V–7.9Cr–5.7Ti	400	150	127	360	20	–	<100	170

The alloy specimens were irradiated in the Fast Flux Test Facility (FFTF), at 420, 520, and 600°C to neutron fluences (E > 0.1 MeV) ranging from 3.7 x 10^{22} n/cm^2 (≈18 displacements per atom, or dpa) to 6.4 x 10^{23} n/cm^2 (≈31 dpa). Helium in the alloy specimens was produced by utilizing transmutation of controlled amounts of ^{6}Li and a predetermined amount of tritium–doped vanadium mother alloy immersed in ^{6}Li + ^{7}Li.[22–24] Table 2 summarizes the actual postirradiation parameters determined from tensile and disk specimens of the V–4Cr–4Ti alloy, i.e., dose and helium and tritium content measured shortly after the postirradiation tests. Helium and tritium were determined by mass spectrometry at Rockwell International Inc., Canoga Park, California.

Table 2. Summary of irradiation parameters of dynamic helium charging experiment, and helium and tritium content of V–4Cr–4Ti specimens

Capsule ID No.	Irradiation Temp. (°C)	Total Damage (dpa)	Calculated Helium (appm) to dpa Ratio[a] at EOI[b] (Assumed k_a or k_w)[c] k_a=0.073 (k_w=0.01)	Measured Helium Content[d] (appm)	Actual Helium–to–dpa Ratio (appm/dpa)	Measured Tritium Content[e] (appm)
4D1	425	31	3.8	11.2–13.3	0.39	27
4D2	425	31	2.8	22.4–22.7	0.73	39
5E2	425	18	2.1	3.3–3.7	0.11	2
5D1	500	18	4.4	14.8–15.0	0.83	4.5
5E1	500	18	3.1	6.4–6.5	0.36	1.7
5C1	600	18	1.1	8.4–11.0	0.54	20
5C2	600	18	1.1	74.9–75.3	4.17	63

[a] L. R. Greenwood "Revised Calculations for the DHCE," April 30, 1993.
[b] Beginning of irradiation (BOI) May 27, 1991; end of irradiation (EOI) March 19, 1992; 203.3 effective full power days (EFPD), hot standby at ≈220°C until November 1992.
[c] Equilibrium ratio (k_a by atom, k_w by weight) of tritium in V alloy to that in the surrounding liquid lithium.
[d] Measured June 1994.
[e] Measured August 1994.

The retrieved TEM specimens, which contained helium, tritium, and neutron displacement damage, were cleaned ultrasonically in alcohol prior to density measurement and microstructural analysis. Most of the examined TEM disks were not degassed at 400°C for 1 h, a customary procedure to expel tritium and hydrogen from Charpy–impact and tensile specimens. Several TEM disks were examined after degassing, but none indicated an appreciable difference in void or helium bubble distribution and microstructure from undegassed specimens that should contain tritium and hydrogen in addition to helium. The irradiated specimens were jet-thinned for TEM in a solution of 15% sulfuric acid-72% methanol-13% butyl cellosolve maintained at -5°C. TEM was conducted with a JEOL 100CX-II scanning transmission electron microscope operating at 100 keV, or with a Philips CM-30 analytical electron microscope operating at 200 keV. Density change was determined from specimen weights measured in air and in research-grade CCl_4.

VOID STRUCTURE AND DISTRIBUTION

A summary of microstructural characterization of voids in the DHCE specimens is given in Table 3. Appreciable numbers of voids in the DHCE specimens were absent, except for specimens retrieved from Capsules 4D1 and 4D2, which were irradiated at 425°C. In specimens irradiated at 600°C and retrieved from Capsules 5C1 and 5C2, only a few helium bubbles were observed at interfaces between the grain matrix and a limited number of Ti(O,N,C) precipitates. TEM images of these microstructural characteristics were reported previously.[27]

Table 3. Summary of void distribution in V–4Cr–4Ti irradiated in the DHCE.

Capsule ID No.	Irradiation Temp (°C)	Total Damage (dpa)	Helium–to–dpa Ratio (appm/dpa)	Voids in Grain Matrix	Voids on Boundary of Grain Matrix and Ti(O,N,C)	Voids on Grain Boundaries
non–DHCE	425, 500, 600°C	24–34	–	none	none	none
4D1	425	31	0.39	some	some	some
4D2	425	31	0.73	some	some	some
5E2	425	18	0.11	none	none	none
5D1	500	18	0.83	none	some	none
5E1	500	18	0.36	none	some	none
5C1	600	18	0.54	none	some	none
5C2	600	18	4.17	none	some	none

Specimens irradiated to 18–31 dpa at 425°C–600°C in the other three capsules (Capsule 5E2, helium generation rate of 0.11 appm He/dpa; 5D1, 0.83 appm He/dpa; and 5E1, 0.36 appm He/dpa) exhibited microstructural characteristics essentially similar to those of specimens from Capsule 5C1 and 5C2, i.e., no helium bubbles either in the grain matrix or on grain boundaries, a few helium bubbles on the interface between the grain matrix and a limited number of Ti(O,N,C) precipitates, and ultrafine Ti_5Si_3 precipitates in high density (only in specimens irradiated at 500°C–600°C). In these specimens, virtually all of the dynamically produced helium atoms seem to have been trapped in the grain matrix without significant bubble nucleation or growth.

For DHCE specimens irradiated to 31 dpa at 425°C in high–tritium capsules 4D1 (helium generation rate ≈0.4 He/dpa) and 4D2 (helium generation rate of ≈0.73 He/dpa), helium bubbles (≈5 nm in diameter) were observed in the grain matrix and on ≈15% of the grain boundaries. Helium bubbles observed near grain boundaries in these specimens were characterized by (a) diffuse bubbles in a number density significantly lower than that of the compact coalescences of helium bubbles observed in other alloys irradiated in tritium–trick experiments;[7–12] (b) discontinuous (≈15% of grain boundaries), in contrast to continuous (≈100% of grain boundaries) coalescence observed in tritium–trick experiments;[7–12] and (c) more or less similar bubble distribution in the grain matrix and near grain boundaries, in contrast to virtual concentration of all helium bubbles on grain boundaries in tritium–trick experiments. These observations seem to indicate that most of the helium atoms produced dynamically at 425°C were trapped in the grain matrix, preventing extensive formation of a continuous coalescence of helium bubbles on grain boundaries. Figure 1 shows typical microstructures of the diffuse helium bubbles in the grain matrix and near grain boundaries and helium shells surrounding Ti(O,N,C) precipitates in specimens irradiated at 425°C (helium generation rates 0.4–0.8 appm He/dpa).

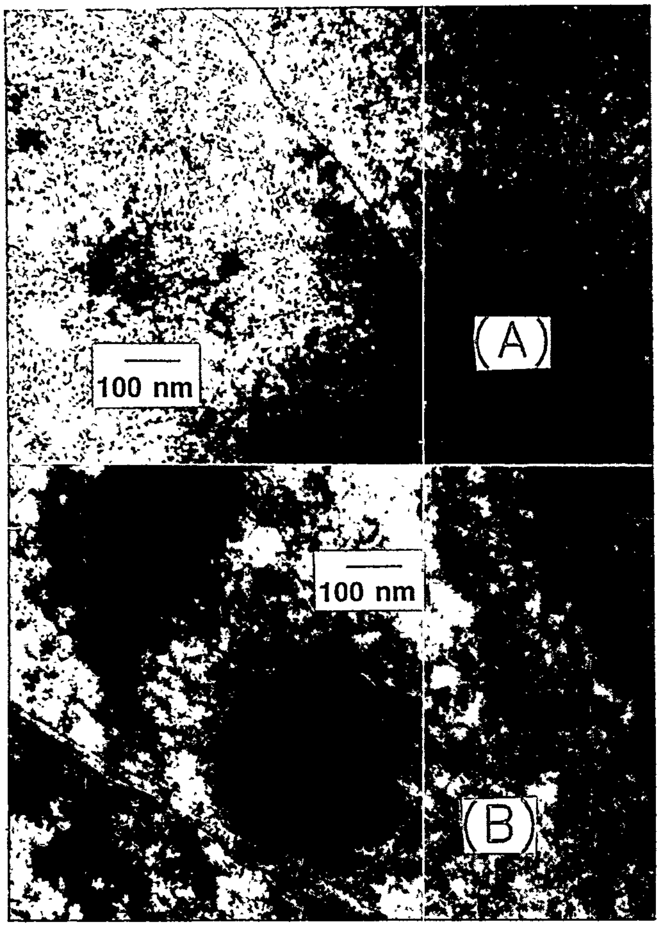

Figure 1.
Void microstructure of V-4Cr-4Ti irradiated at 425°C to ≈31 dpa in DHCE (Capsules 4D2 and 4D1): (A) similar distribution of diffuse voids in grain matrices and near grain boundary; and (B) limited number of voids near grain boundary and void shells surrounding Ti(O, N, C).

As in non–DHCEs,[4] Ti_5Si_3 did not precipitate during irradiation at 425°C in the DHCEs. If Ti_5Si_3 precipitation was indeed significant for 425°C irradiation, void swelling at that temperature would have been suppressed significantly, as in other alloys irradiated at 420°C in non–DHCEs.[28]

DENSITY CHANGE

Results of density measurements for specimens irradiated at 600 (18 dpa in Capsule 5C1) and 425°C (18 dpa in Capsule 5E2, 31 dpa in Capsules 4D1 and 4D2) are given in Figs. 2A and 2B, respectively. The helium generation rates in the DHCE specimens are also given in the figure (see Table 2). For comparison, density changes determined for similar irradiation conditions in non–DHCEs[3] are also shown in the figures.

Density changes in the non–DHCE and DHCE specimens irradiated at 500°C and 600°C were low (<0.6 %). The small density change seems to be consistent with the negligible number density of voids or helium bubbles (Table 3).[27] However, density changes in the DHCE specimens irradiated at 425°C (Capsules 4D1, helium generation rate ≈0.4 He/dpa and 4D2, helium generation rate ≈0.73 He/dpa) were somewhat higher than those of the non–DHCE specimens. The relatively large density changes measured for these specimens seem also to be consistent with the relatively higher number density of helium bubbles (Fig. 1).

Density changes measured in disk specimens of V–5Ti, V–3Ti–1Si, and V–8Cr–6Ti, irradiated to ≈18 dpa at 425°C in a DHCE in Capsule 5E2, are shown in Fig. 3. In the figure, density changes in the DHCE are compared with those obtained on similar specimens irradiated to ≈34 dpa in a non–DHCE. Although the helium content of these alloy specimens was not measured, the actual helium generation rate was expected to be low and similar to that of V–4Cr–4Ti (i.e., 0.11 appm He/dpa). Effects of helium on density changes in these alloy specimens were insignificant.

DISCUSSION

Microvoids or helium bubbles were absent from all of the specimens of V–4Cr–4Ti irradiated in the DHCE at 500–600°C, except for a few helium bubbles at interfaces between the grain matrix and some Ti(O,N,C) precipitates that are normally present in V–Ti and V–Cr–Ti alloys. Preferential formation of voids near blocky precipitates [presumably Ti(O,N,C) precipitates] was also reported by Braski in V–3Ti–1Si specimens that were preimplanted with 82 appm helium by the tritium–trick technique and then irradiated to 40 dpa at 600°C.[8]

Buitenhuis et al. proposed that interfaces between the grain matrix and Ti(O,N,C) precipitates act as preferential sinks for helium.[29] From a series of thermal desorption analyses by mass spectroscopy, these authors have identified a helium desorption peak at the surprisingly low temperature of ≈280°C in V–5Ti specimens that were irradiated and implanted with helium ions. Some of the desorption peaks were sharp and narrow and some were weak and broad below and above ≈280°C. Furthermore, Buitenhuis et al. attributed the former and the latter types of peaks to helium–vacancy–impurity (O, N, and C) complexes that are produced in the grain matrix and near the interfaces between the grain matrix and Ti(O,N,C) precipitates, respectively, and are subsequently dissociated into helium and vacancy–impurity complexes upon heating to ≈280°C or higher. During our degassing treatment in which DHCE specimens were heated to ≈405°C at a linear rate of 0.2°C/s in high vacuum in the present study, desorption peaks were observed consistently at ≈280°C. However, a positive identification of helium desorption was not made from a mass spectroscopic analysis.

One of the important findings from the DHCE was that the actual (measured) helium and tritium content of V–4Cr–4Ti specimens was significantly lower than that calculated on the basis of the assumed equilibrium ratio (k_w = 0.01) of tritium in the alloy to that in the liquid lithium (Table 2). This could be interpreted to indicate that k_w is significantly lower than previously thought, in particular for irradiations at 425 and 500°C.

Microvoids or helium bubbles were absent in the grain matrix and on grain boundaries in all of the specimens irradiated at 500–600°C, in which ultrafine Ti_5Si_3 precipitated in high density. Even in specimens irradiated at 600°C at the highest helium generation rate of ≈4.2 appm helium/dpa (Capsule 5C2), no microvoids could be detected either in the grain matrix or on grain boundaries. This correlation between the high–density precipitation of ultrafine Ti_5Si_3 and negligible void swelling seems to be consistent with similar observations reported previously for non–DHCE conditions.[28] Conversely, the relatively higher void swelling and larger density change observed in specimens irradiated at 425°C (in Capsule 4D1 and 4D2) seems to be associated with an absence of precipitation of ultrafine Ti_5Si_3 at the low irradiation temperature.

As pointed out above, the characteristics of grain–boundary helium bubbles observed in the specimens irradiated to 31 dpa at 425°C were in distinct contrast to those observed in specimens from tritium–trick experiments, i.e., diffuse bubbles in significantly lower number density than those of the compact coalescences of helium bubbles in tritium–trick experiments; discontinous (on ≈15% of grain boundaries), in contrast to continuous (≈100% of grain boundaries) coalescences in tritium–trick experiments; and similar bubble distribution in the grain matrix and near grain boundaries, in contrast to virtual concentration of all helium bubbles on grain boundaries in tritium–trick experiments. These characteristics seem to indicate that most of the helium atoms produced at 425°C in DHCEs were trapped by vacancies or vacancy–impurity complexes.

Intergranular fracture morphology was not observed in any of the specimens irradiated in the DHCE and subsequently tested by uniaxial tensile tests at 23 to 600°C and multiple bending tests at –196 to 50°C. Even in specimens irradiated at 425°C and fractured in brittle manner during multiple bending tests at –196°, only cleavage and ductile tearing were observed, i.e., intergranular fracture morphology was absent. These observations, consistent with the characteristics of helium bubble distribution described above, are in distinct contrast to the propensity to intergranular fracture that is commonly observed in tritium–trick experiments.

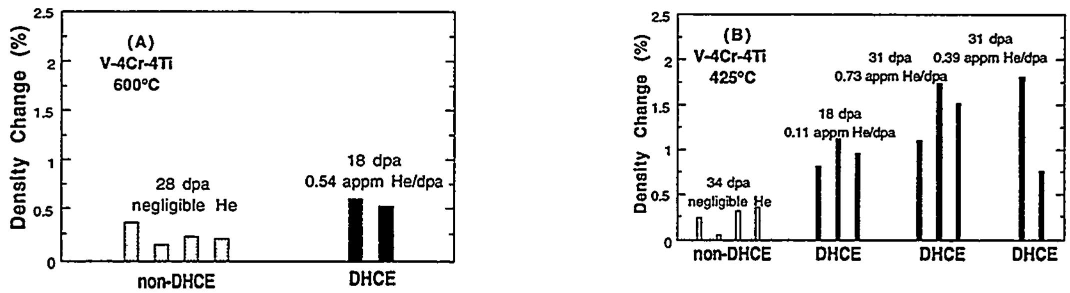

Figure 2. Comparison of density changes of V–4Cr–4Ti from DHCE and non–DHCE experiments: (A) 600°C and (B) 425°C.

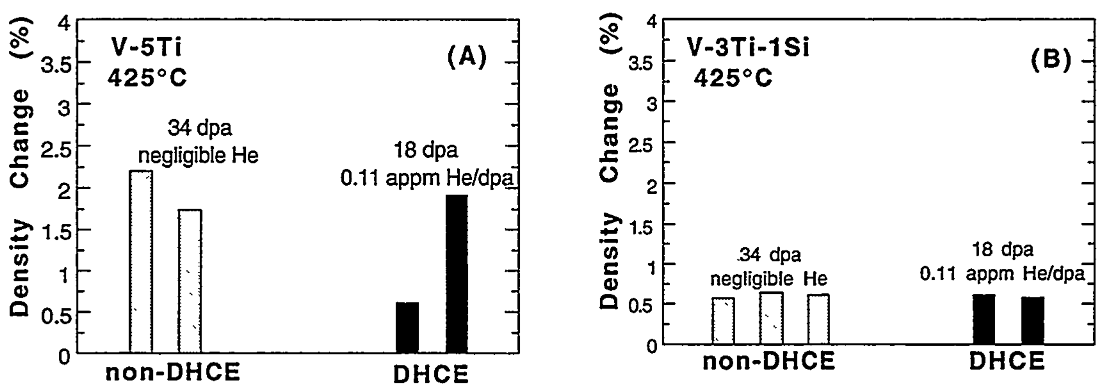

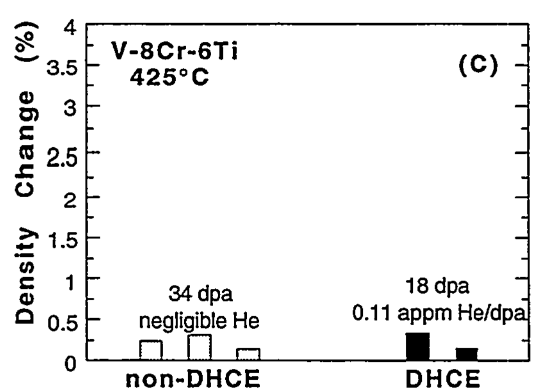

Figure 3.
Density changes of (A) V–5Ti; (B) V–3Ti–1Si; and (C) and V–8Cr–6Ti irradiated at 425°C to 18 dpa in DHCE and to 34 dpa in non–DHCE

CONCLUSIONS

(1) For specimens irradiated to ≈18 dpa at 500–600°C in the Dynamic Helium Charging Experiment (DHCE) with helium generation rates of ≈0.4–4.2 appm He/dpa, void swelling was negligible, and density changes from the DHCE and non–DHCE (negligible helium generation) were similar (<0.6%).

Only limited number of voids or helium bubbles were observed at the interface of the grain matrix and some of the Ti(O,N,C) precipitates. Neither helium bubbles nor voids were observed either in the grain matrix or near grain boundaries. Under irradiation at these temperatures, ultrafine Ti_5Si_3 precipitated in high density and most of the dynamically produced helium atoms seem to be trapped in the grain matrix and at the interface between the matrix and Ti_5Si_3 precipitates, without a significant chance for bubble nucleation or growth.

(2) For DHCE specimens irradiated to 31 dpa at 425°C at helium generation rates of ≈0.4–0.73 appm He/dpa, helium bubbles ≈5 nm in diameter were observed in localized regions of the grain matrix as well as on limited portions (≈15%) of grain boundaries. Grain–boundary helium bubbles in these specimens were diffuse, in contrast to the compact coalescences of helium bubbles observed from tritium–trick experiments; discontinous (near ≈15% of grain boundaries), in contrast to continuous (on ≈100% grain boundaries) coalescence observed in tritium–trick experiments; and more or less evenly distributed in the grain matrix and near grain boundaries, in contrast to virtual concentration of all helium bubbles on grain boundaries in tritium–trick experiments. These observations indicate that most of the helium atoms that were produced dynamically at 425°C were trapped in the grain matrix, preventing formation of continuous coalescence of compact bubbles on grain boundaries. As in non–DHCE, the irradiation–induced precipitation of ultrafine Ti_5Si_3 was not observed after irradiation at 425°C.

(3) Intergranular fracture morphology was not observed in any of the specimens irradiated in DHCEs and subsequently fractured during uniaxial tensile tests at 23 to 600°C and multiple bending tests at −196 to 50°C. This observation, consistent with the characteristic helium bubble distribution, is in distinct contrast to the propensity to intergranular fracture commonly observed in tritium–trick experiments.

(4) The actual measured helium and tritium content of V–4Cr–4Ti was significantly lower than that calculated with an assumed equilibrium ratio (≈0.01 by weight) of tritium in the alloy to that in the liquid lithium. This indicates that the tritium equilibrium ratio is significantly lower than previously assumed, in particular, for irradiations at <500°C. It also indicates that the tritium level in lithium–cooled V–4Cr–4Ti first wall/blanket structures, and hence the effect of tritium on the fracture toughness, will be significantly lower than previously thought.

ACKNOWLEDGMENTS

The successful completion of the complex and difficult Dynamic Helium Charging Experiment was possible through many years of contributions from F. W. Wiffen, H. Matsui, K. Abe, C. E. Johnson, R. G. Clemmer, J. P. Kopasz, L. R. Greenwood, M. L. Hamilton, K. L. Pearce, R. Ermi, A. Ermi, H.–C. Tsai, and R. V. Strain. The authors are grateful to L. R. Greenwood and B. M. Oliver for calculation and measurement, respectively, of helium and tritium contents.

REFERENCES

[1] B. A. Loomis, L. Nowicki, and D. L. Smith, "Effect of Neutron Irradiation on Tensile Properties of V–Cr–Ti Alloys," in Fusion Reactor Materials, Semiannual. Prog. Report, DOE/ER-0313/15, Oak Ridge National Laboratory, Oak Ridge, TN (1994), pp. 219–222.

[2] B. A. Loomis, H. M. Chung, L. Nowicki, and D. L. Smith, "Effects of Neutron Irradiation and Hydrogen on Ductile-Brittle Transition Temperatures of V–Cr–Ti Alloys," ibid., pp. 253–257.

[3] H. M. Chung, B. A. Loomis, L. Nowicki, J. Gazda, and D. L. Smith, "Irradiation-Induced Density Change and Microstructural Evolution of Vanadium-Base Alloys," ibid., pp. 223–231.

[4] H. Matsui, M. Tanno, J. Gazda, and H. M. Chung, "Microstructural Stability of V-4Cr-4Ti During Neutron Irradiation," ibid., pp. 240–246.

[5] H. M. Chung, J. Gazda, L. Nowicki, J. E. Sanecki, and D. L. Smith, "Effects of Fabrication Variables on Impact Properties and Microstructure of V–Cr–Ti Alloys," ibid., pp. 207–218.

[6] H. M. Chung, B. A. Loomis, and D. L. Smith, "Thermal Creep Behavior of V–5Cr–5Ti and V–10Cr–5Ti Alloys," in Fusion Reactor Materials, Semiannual. Prog. Report, DOE/ER-0313/14, Oak Ridge National Laboratory, Oak Ridge, TN (1993), pp. 309-317.

[7] D. N. Braski and D. W. Ramey, in Effects of Radiation on Material Properties, ASTM-STP 870, F. A. Garner and J. S. Perrin, eds., American Society for Testing and Materials, Philadelphia, 1985, pp. 1211–1224.

[8] D. N. Braski, in Influence of Radiation on Material Properties, ASTM-STP 956, F. A. Garner, C. H. Henager, and N. Igata, Eds., American Society for Testing and Materials, Philadelphia, 1987, pp. 271-290.

[9] D. N. Braski, J. Nucl. Mater. 141-143 (1986) 1125.

[10] D. N. Braski, in Reduced Activation Materials for Fusion Reactors, ASTM-STP 1047, Philadelphia (1988), pp. 161-178.

[11] H. Matsui, M. Tanaka, M. Yamamoto, and M. Tada, J. Nucl. Mater. 191-194 (1992) 919.

[12] M. Satou, K. Abe, and H. Matsui, J. Nucl. Mater. 191-194 (1992) 938.

[13] M. Tanaka and H. Matsui, Mater. Trans., JIM, 34 (1993) 1083.

[14] W. van Witzenburg, A. Mastenbroek, and J. D. Ellen, J. Nucl. Mater. 103-104 (1981) 1187.

[15] M. P. Tanaka, E. E. Bloom, and J. A. Horak, J. Nucl. Mater. 114 (1981) 895.

[16] M. L. Grossbeck and J. A. Horak, in Influence of Radiation on Material Properties, ASTM-STP 956, Philadelphia (1986) 291.

[17] J. M. Vitek, D. N. Braski, and J. A. Horak, J. Nucl. Mater. 141-143 (1986) 982.

[18] W. van Witzenburg and E. de Vries, in Effects of Radiation on Materials, ASTM-STP 1125, Philadelphia (1990).

[19] L. L. Horton and K. Farrell, J. Nucl. Mater. 122-123 (1984) 687.

[20] H. Kawanishi and S. Ishino, in Reduced Activation Materials for Fusion Reactors, ASTM-STP 1047, Philadelphia (1988), pp. 179-189.

[21] H. Kawanishi, Y. Arai, and S. Ishino, J. Nucl. Mater. 191-194 (1992) 933.

[22] D. L. Smith, H. Matsui, L. R. Greenwood, and B. A. Loomis, J. Nucl. Mater. 155-157 (1988) 1359.

[23] D. L. Smith, B. A. Loomis, H. Matsui, M. L. Hamilton, K. L. Pearce, J. P. Kopasz, C. E. Johnson, R. G. Clemmer, and L. R. Greenwood, in Fusion Reactor Materials, Semiannual. Prog. Report. DOE/ER-0313/10, Oak Ridge National Laboratory, Oak Ridge, TN (1991), p. 159.

[24] H. Tsai, H. M. Chung, B. A. Loomis, and D. L. Smith, "Status of Dynamic Helium Charging Experiment (DHCE)," in Fusion Reactor Materials, Semiannual. Prog. Report. DOE/ER-0313/15, Oak Ridge National Laboratory, Oak Ridge, TN (1994), p. 247.

[25] H. M. Chung, B. A. Loomis, L. Nowicki, and D. L. Smith, "Effect of Dynamically Charged Helium on Tensile Properties of V–4Cr–4Ti," in this report.

[26] M. Satou and H. M. Chung, in Fusion Reactor Materials, Semiannual Prog. Rep. DOE/ER-0313/13, Oak Ridge National Laboratory, Oak Ridge, TN (1993), p. 227.

[27] H. M. Chung, B. A. Loomis, H. Tsai, L. Nowicki, J. Gazda, and D. L. Smith, "Swelling and Structure of Vanadium Alloys Irradiated in the Dynamic Helium Charging Experiment," in Fusion Reactor Materials, Semiannual. Prog. Report, DOE/ER-0313/16, Oak Ridge National Laboratory, Oak Ridge, TN (1994), in press.

[28] H. M. Chung, B. A. Loomis, and D. L. Smith, in Effects of Radiation on Materials, ASTM-STP 1175, A. S. Kumar, D. S. Gelles, R. K. Nanstad, and T. A. Little, Eds., American Society for Testing and Materials, Philadelphia, 1993, pp. 1185–1200.

[29] T. Buitenhuis, A. Fedorov, and A. van Veen, "Thermal Desorption Investigation of V–5Ti Alloy," IRI–131–94–005, Delft University of Technology Report, The Netherlands, 1994.